A web-based histology atlas for the freshwater Cladocera species *Daphnia magna*

Short title: Web-based *Daphnia* histology atlas

Mee S. Ngu[1,2], Daniel J. Vanselow[1,2], Carolyn R. Zaino[1,2], Alex Y. Lin[1,2], Jean E. Copper[1,2], Margaret J. Beaton[3], Luisa Orsini[4], John K. Colbourne[4], Keith C. Cheng[1,2,*], Khai C. Ang[1,2,*]

[1]Department of Pathology, Pennsylvania State University College of Medicine, Pennsylvania, USA

[2]Jake Gittlen Laboratories for Cancer Research, Pennsylvania State University College of Medicine, Pennsylvania, USA

[3]Department of Biology, Mount Allison University, Sackville, Canada

[4]Centre for Environmental Research and Justice, The University of Birmingham, Birmingham, UK

*Equal, contributing corresponding authors:

Khai C. Ang (kca2@psu.edu)

Keith C. Cheng (kcheng76@gmail.com)

Abstract

Daphnia are keystone species of freshwater habitats used as model organisms in ecology and evolution. They are also routinely used as environmental sentinels in regulatory toxicology and are increasingly contributing to new approach methodologies (NAM) for chemical risk assessments Yet, it is challenging to establish causal links between biomolecular (omics) responses to chemical exposure and their toxicity phenotypes without a baseline knowledge of tissue- and cell-morphology of healthy individuals. Here, we introduce the *Daphnia* Histology Reference Atlas (DaHRA, http://daphnia.io/anatomy/), which provides a baseline of wildtype anatomical and microanatomical structures of female and male *Daphnia magna*. This interactive web-based resource features overlaid vectorized demarcation of anatomical structures that compliant with an anatomical ontology created for this atlas. Since sex is environmentally induced in *Daphnia*, DaHRA is a map of sexual dimorphism by phenotypic plasticity. We also benchmark this tool for mechanistic toxicology by exposing *Daphnia* to acetaminophen and use the atlas to document its effects in organs, tissues, and cell-types. DaHRA represents an essential step towards correlating phenotypes with the discovery power of hypothesis-free, molecular backdrop against which pathology can be interpreted, thereby offering a platform to elucidate how genetic variation and external perturbations cascade through multiple biological scales to influence phenotype.

Keywords: *Daphnia magna*, histology, microanatomy atlas, phenotypes, sexual dimorphism, histopathology

Synopsis: Whole-organism *Daphnia* atlas as foundation for unbiased phenotyping, and its utility in characterizing sexual dimorphism and effects of chemical toxicity.

1. Introduction

Despite regulatory restrictions on hazardous chemicals, chemical pollution is the leading cause of premature deaths and morbidities globally (1–3). Adding to this, habitat loss, climate change, and pollution are also leading environmental factors impacting biodiversity, with more than 60% of ecosystems services being reduced or wiped out in the last two decades (4). The introduction

of new approach methodologies (NAMs) for assessing chemicals for their toxicity is designed to improve regulatory outcomes by replacing outdated, data-poor methods that rely on observing apical endpoints (such as death or reproductive failure in selected animals) with modern methods at revealing the pathways to toxicity (5) These methods include data-rich techniques such as transcriptomics and metabolomics (omics) that measure changes in the abundance of all gene transcripts and endogenous metabolites upon exposure that are indicative of the chemical modes of action (6–8). Although these data are robust at measuring biomolecular activity linked to a huge array of potential adverse health effects, these data must be anchored to their phenotypic effects for regulatory relevance (9). Yet despite omics producing high content mechanistic information that enables data-driven discoveries, there are few analogs to discover causal links to phenotypes. A primary objective of this paper is to provide a necessary resource for obtaining and interpreting high content phenotypic data for the model species *D. magna*, which is used globally to set regulatory limits on potentially hazardous chemical substances in the environment and one of five models used uncover the evolutionary origins of toxicity (10).

The water flea *Daphnia* is a keystone branchiopod crustacean (order Cladocera) in freshwater lotic ecosystems worldwide and is an established model in ecology, evolution, and ecotoxicology (11–13). They are responsive to environmental change and they adapt via evolutionary mechanisms and plasticity (14–16). This plasticity includes the sex of daphniids, which is determined by environmental conditions. Relevant to ecotoxicity testing is their short generation time that enables the experimental manipulation of large populations; and a parthenogenetic life cycle that allows the rearing of populations of identical clones from single genotypes (17). The latter property has the unique advantage of allowing the concurrent study of molecular and phenotypic responses to multiple environmental insults, including chemical pollutants. *Daphnia magna* is the species of choice in ecotoxicogenomics (18,19). Recently, its hologenome (20), reference genome (21,22) and transcriptome (23–25) have been published, elevating this species to the ranks of other biomedical model species for ecological genomics. Yet, the full potential of this species cannot be entirely realized without the correlation between molecular, and tissue- and cell- specific phenotypic responses.

Histopathology, the histological study of tissue-specific changes, enables the identification of targets of toxicity and diseases, bridging phenotypes and biomolecular perturbations induced by environmental insults (26,27). Histopathology-based toxicological studies in fish (28–30) and bivalves (31,32) have shown to be useful for water quality monitoring and assessment. The application of histopathology to millimeter-size sentinel species used in ecotoxicology would enable the analysis of tissue-specific toxicity phenotypes in the whole animal. However, identification of affected cell and tissue types requires prior knowledge of normal structure, which is generally only possible through atlases.

Here, we present the first curated web-based histology atlas for both female and male *D. magna*, further broadening the discovery capacity of this sentinel species. We optimized methods for *D. magna* histology and created a collection of digitized histological images for adult female and male *D. magna* in three anatomical planes to elucidate sexual dimorphism by environmentally induced phenotypic plasticity. We included the first proof-of-concept application of this atlas by comparing tissue of clonal replicates of the same genotype of *D. magna* under control conditions (no chemical exposure) with replicates exposed to an over-the-counter painkiller, acetaminophen. This common pharmaceutical substance is found in surface waters and wastewater throughout the world (33). Besides its therapeutic effects, it is known to induce toxicological outcomes if overdose (34,35). This benchmarked resource for mechanistic toxicology using *Daphnia* is made open-access and interactive, allowing smooth magnification with a dynamic scale bar. Anatomical structures are highlighted and labeled corresponding with an anatomical ontology, providing researchers and chemical risk managers with an unprecedented tool to navigate both normal and abnormal microanatomical structures of organs, tissues, and cell-types. This resource has the potential to support tissue-specific and whole-organism phenotyping, informing (eco)toxicology, genetics and phenomics studies.

2. Material and methods

2.1 *Daphnia magna* culturing

A commercial strain of *D. magna* was purchased from Carolina Biological (NC, USA) and raised in "Aachener Daphnien-Medium" or ADaM at room temperature (20°C ± 1°C) under a 16-hour

light/8-hour dark photoperiod. *D. magna* cultures were fed three times weekly with 3.0 x 10^7 cells/ml of green microalgae (*Raphidocelis subcapitata)* and once a week with 0.1 mg/mL of dissolved bakers' yeast. The animal density was maintained at about 20 neonates, 10 juveniles and 6 to 8 reproducing adults per liter to prevent overcrowding. Under these conditions, animals reached maturity at 6 to 8 days post-birth and reproduced parthenogenetically every 3 days after sexual maturation with an average of 15 neonates per brood from the second brood onwards. Production of males was induced by overcrowding (>10 reproducing adults per liter) and shorter photoperiod (8 hours) (36).

2.2 Chemical Exposure

Reproducing female *D. magna* (approximately 10 days old and carrying the second parthenogenetic brood 2 hours post-ovulation) were exposed to 5 concentrations of acetaminophen (5, 15, 25, 35, 50 mg/L). Gravid *D. magna* were used for this exposure to evaluate the toxic effects of acetaminophen on both adults and developing embryos. The exposures lasted for 72 h and were conducted with two adult females in 200 ml medium. The medium was replenished, and the animals fed daily. After 72 h exposure, each surviving animal was prepared for histological observations as described in the following.

2.3 Histological Processing

2.3.1 Fixation and decalcification

Exposed and control clones of *D. magna* were fixed with 20X Bouin's solution (Newcomer Supply, WI) and incubated for 48 h at room temperature (about 21°C) on a low-speed orbital shaker (Corning LSE) set to 55 revolutions per minute (RPM). The fixation is done to preserve tissues from decay due to autolysis or putrefaction. After the fixation step, samples were washed twice with 1X phosphate-buffered saline (PBS) for 10 min. This washing step was followed by decalcification in 20X sample volume of pre-chilled 6% formic acid (Sigma-Aldrich, MO) for 24 h on the orbital shaker set to 55 RPM. Samples were then rinsed in 70% ethanol for one minute and immersed in fresh 70% ethanol for 30 min before agarose embedding. Different fixation methods were compared before opting for the Bouin's solution. We tested fixation using 4% Paraformaldehyde in 0.1M phosphate buffer (pH 7.4) (Bioenno LifeSciences, CA) and 10%

Buffered Formalin Phosphate (Fisher Scientific, ON) with different fixation times and temperatures (Supplementary Table 1).

2.3.2 Agarose embedding

Agarose embedding using a mold or an array facilitates consistent positioning and orientation of millimeter-size samples for sectioning (37,38). Adapted from Sabaliauskas et al. (2006)(39), a mold was designed and 3D -printed for casting an agarose block with wells that could hold up to 18 adult *D. magna* for concurrent tissue processing and sectioning . To create an agarose block, laboratory labeling tape (VWR) was wrapped tightly around the mold. Then, 2.5 mL of 1 % agarose (Sigma-Aldrich, MO) at 55 °C was pipetted onto the mold and allowed to solidify at room temperature. The agarose block was removed gently from the mold. Each fixed *D. magna* sample was pipetted with a small volume of ethanol and transferred into the well of the agarose block using a single-use plastic transfer pipette. Samples designated for the sagittal plane sectioning were laid on their sides with a swimming antenna in the wells and all rostra facing the same direction (see Supplementary Figure 1 for *Daphnia* anatomy and Supplementary Text 1 for *Daphnia* anatomy glossary). Samples designated for coronal and transverse orientation were laid on their back in the wells. Once all samples were positioned in individual wells, excess ethanol was carefully dried off using lint-free Kimwipes without touching the samples. Each sample was first topped-off with one drop of molten 1 % agarose (about 50 °C) without disturbing the sample, followed by a thin layer of 1% agarose to completely cover the sample. After the agarose layer solidified (about 5 min at room temperature), the block was trimmed as needed, placed into a tissue cassette, and stored in 70 % ethanol for tissue processing.

2.3.3 Tissue processing, sectioning, and staining

All samples were dehydrated in graded ethanol and infiltrated with Formula R paraffin (Leica Biosystems #3801450) in RMC Model 1530 automated closed reagent type tissue processor (Supplementary Table 2). Following this step, they were serially sectioned at 5 µm on a Leica RM2255 automated rotary microtome. Sections were then stained with Harris' hematoxylin and eosin in an auto-stainer (Sakura Tissue Tek DRS 2000, IMEB, CA) following a protocol adapted from Copper et al. (2018) (40) where the duration of hematoxylin staining was extended from 3

to 7 min to achieve better contrast for samples fixed with Bouin's solution (Supplementary Table 3). Cover glasses No. 1 (Platinum Line) were used for cover-slipping.

2.4 Histology slide digitization

All slides were screened using an Olympus BX41 microscope and 10X and 20X objective lenses. Those selected for the atlas were scanned at 40X using an Aperio AT2 slide scanner (Leica Biosystems, IL) and images were saved in TIFF format. 40X scanning was performed using 20X objective lens (0.075 n.a. Plan Apo) with 2X optical magnification changer, yielding a digital resolution of 0.25-micron per pixel. The images of *D. magna* samples included in the atlas were cropped using Aperio ImageScope (version 12.4.3.5008). Three channels (Red, Green, Blue) of these digital slides were stacked using Fiji (41) or ImageJ (42). Then, image processing was performed in Adobe Photoshop (version 22.1.1) where images were rotated and set to have the same canvas size; the image background was removed using "Remove Background"; the "Exposure" was adjusted to fall between 0.1 to 0.25 and the same value was used for each set of images; and "Levels" were adjusted using preset "Midtones Darker". Each set of digital slides was then pyramidally tiled for the web-based viewer.

2.5 Digital labeling of anatomical structures

The anatomical ontology, consisting of a list of anatomical terms organized by groups (organ systems) and subgroups (tissues and cell types), was created for the atlas (Supplementary File 1). We cross-referenced the extensive work of Fryer (43) with other published literature (44–70) and decided on the commonly used *Daphnia* anatomical terms. Annotation and labels for each anatomical structure presented on the atlas were created using Adobe Illustrator (version 25.1). One image at a time, each anatomical structure was annotated by outlining the structure using the "Curvature" and assigned a color corresponding with the anatomical ontology. Annotation and labels of each structure were saved under "Layers". After completion of the labeling of all anatomical structures on a given image, the annotation was exported in a single scalable vector graphic (SVG) to be used as input for the web-based viewer.

2.6 Building the web-based digital slide visualization platform

The file size of a set of digitized images is > 4 GB, making access challenging for users with standard computational resources. To improve accessibility and usability we developed an open-access, web-based digital slide viewing platform based on the open-access project OpenSeadragon (https://openseadragon.github.io/). This interface removes the need to download full-resolution images. The viewer combined annotations and digital scans into a seamless experience to provide user-friendly access to high-resolution data. The atlas' code was written in client-side JavaScript, HTML, and CSS. Pyramidally tiled images were parsed and visualized with OpenSeadragon. When the user opens an image, the viewer will open the corresponding SVG file containing all the anatomical labels and their corresponding shape vector information. The viewer parses all labels from the SVG file, plotting the corresponding regions, and updates the ontology to note which regions are available to visualize on a particular image.

3. Results and discussion

3.1 *Daphnia magna* histology atlas presenting *Daphnia* microanatomy and enabling the discovery of aberrant phenotypes

3.1.1 Interactive viewer for *Daphnia* Histology Reference Atlas (DaHRA)

We developed the *Daphnia* Histology Reference Atlas (DaHRA; http://daphnia.io/anatomy/), a user-friendly interface to access a collection of digitized histological sections, including wildtype female and male *D. magna* in three standard anatomical planes (Figure 1), and *D. magna* exposed to 25 mg/L acetaminophen (Figure 2; http://daphnia.io/anatomy/treatments/).

The interface allows users to visualize digital scans (0.25-micron per pixel resolution) with and without annotations of anatomical structures. The anatomical ontology (Supplementary File 1) including of all the anatomical structures can be found on the left side of the viewer, with the anatomical terms arranged alphabetically within 8 groups: circulatory, digestive, excretory, locomotive and respiration, muscular, nervous, sensory and vision, post-abdomen, and reproductive (Figure 1B). Annotations of the anatomical structures are presented as color overlays and indicated by check marks next to the anatomical terms. Unchecking the box hides

the color overlays. Anatomical terms with underlined labels indicate nested substructures (for example, “microvilli” under “epithelial cell”, both under “midgut”). Hovering over an anatomical term in the ontology dynamically highlights the corresponding structure or structure groups in the viewer, temporarily hiding other checked structures. A collection of abnormal anatomical structures of *D. magna* exposed to 25 mg/L acetaminophen is shown under “Histopathology” (Figure 2B).

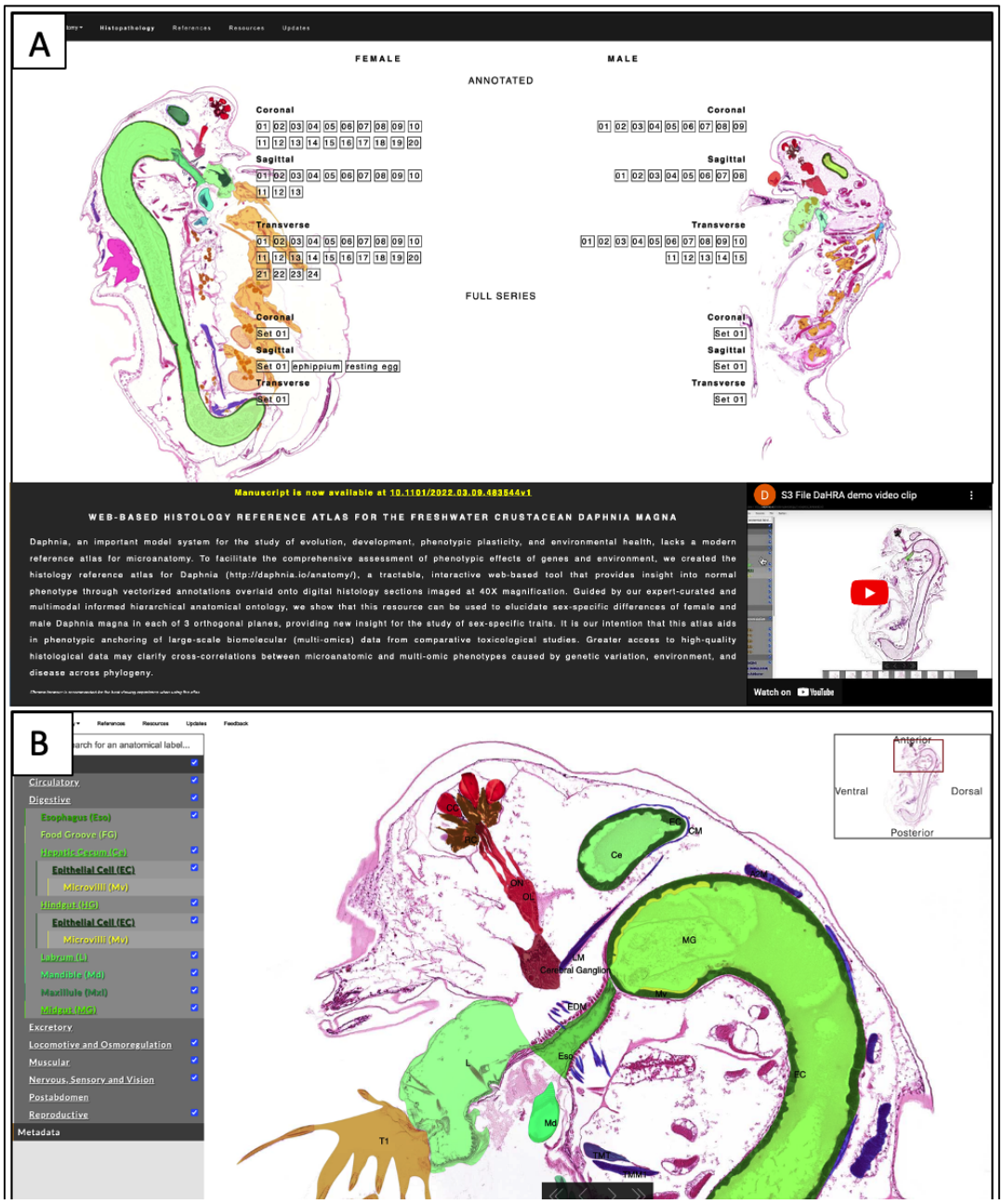

Figure 1. Overview of the interactive web-based viewer for DaHRA. (A) Landing page hosting all annotated and unannotated histology images of the same female and male strain of *D. magna* with an instruction video describes the features of the atlas. **(B)** Interactive viewer displaying the expandable list of anatomical structures on the left; the checked boxes indicate the structures labeled in the image. The anatomical terms on the image are shown as acronyms; hovering the mouse cursor over an acronym or its corresponding region will show the full term. Unchecking a box will hide the color overlay and annotation corresponding to the box.

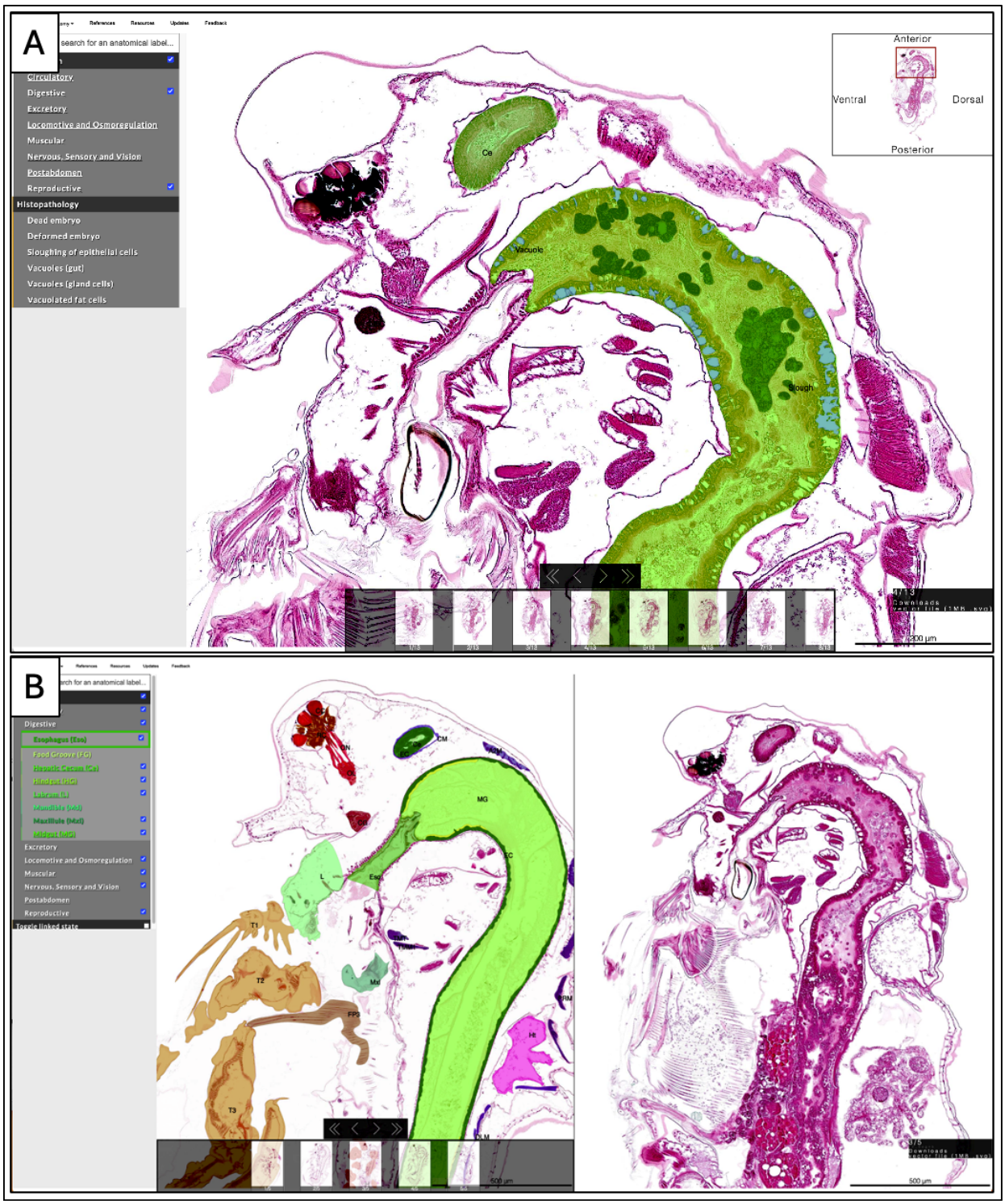

Figure 2. Overview of the atlas displaying annotated histopathological data. (A) The checked boxes in the anatomical ontology indicate the affected structures overlaid with annotation and the observed abnormalities listed under "histopathology". **(B)** Viewer comparing the non-exposed (left) to the acetaminophen-exposed (right) *D. magna*.

3.1.2 *Daphnia magna* male and female microanatomy

DaHRA presents the first microanatomical representation of female and male *D. magna* from the same genotype. All organs and cell types included in the anatomical ontology are briefly described here with representative images from the three anatomical planes of the female (Figure 3A-C) and male *D. magna* (Figure 3D-F). The terminology used for the DaHRA anatomical ontology (a list of terms organized by groups and subgroups) was cross-referenced with published literature (43–69) for uniformity. We identified 50 anatomical structures, and categorized them in 8 groups (circulatory, digestive, excretory, locomotive and respiration, muscular, nervous, sensory and vision, postabdomen, and reproductive), and can be expended if/ when more structures are identified.

Here, we first summarize the sexually dimorphic traits in *D. magna* and follow with a brief description of the normal anatomy and microanatomy. Apart from the obvious differences in body size and reproduction organs, *D. magna* presents other sexual dimorphisms that can be clearly visualized and compared on the atlas. Generally, the body size and first antennae or antennules of *D. magna* differ between the sexes. Adult males have a smaller body size but much longer antennules bearing a single long peg or flagellum on the tip (Figure 3D'). Male antennules are also composed of muscle tissue (Figure 3D) that is absent in females. The first thoracic limbs of the males are equipped with elongated setae (Figure 3E) and chitinized copulatory hooks (Figure 3F) that are used for clasping females during copulation. The male postabdomen has gonopores (Figure 3D inset) that are involved in transferring mature spermatozoa from the testes to the female in the region of the oviduct during copulation. Besides having a wider frontal opening, pubescence and thickened angular margins are also observed at the ventral margin of the carapace in males (indicated by arrows in Figures 3E and 3F). Fat cells in males are different from those found in females. Male fat cells contain much larger lipid droplets, reduced and less granular cytoplasm, and smaller nucleoli than female fat cells (Figure 4).

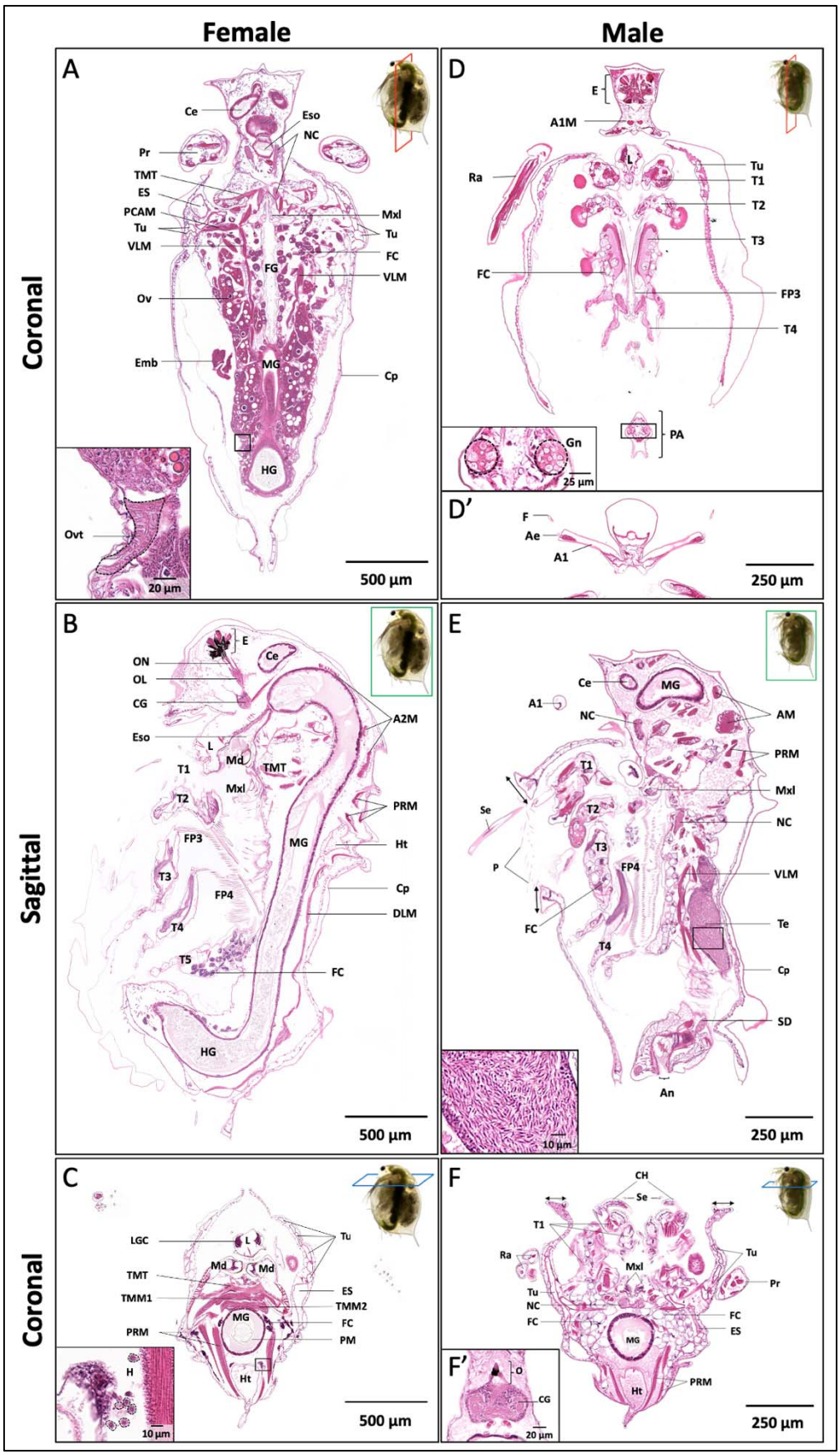

258

Figure 3. Representative microanatomical structures of female (A-C) and male (D-F') *D. magna* in the three orthogonal planes. The coronal plane (panel A and D) displays most of the structures in pairs. Inset of panel A shows the oviduct (Ovt; dotted circle) and inset of panel D shows gonopores (Gn) in the male. Panel D', slightly ventral to panel D, displays the prominent and elongated antennules (A1) with flagella (F) at the tips. The sagittal plane of the female (panel B) displays the connection of the compound eye (E) to the optic lobe (OL) and cerebral ganglia (CG) by optic nerves (ON). The labrum (L), maxillules (Mxl), and mandibles (Md) are anterior to the esophagus (Eso) that opens into the midgut (MG) and is followed by the hindgut (HG). This section also cuts through the five thoracic limbs (T1-5) and filter plates (FP3, FP4). The sagittal plane of the male (panel E) shows the elongated seta (Se) on the first thoracic limb, pubescence (P) at the wider ventral opening of the carapace, thickening of carapace at the ventral opening (arrows), one of the testes (Te), and a small portion of sperm duct (SD). Inset of panel E showing the spermatozoa in the testis. The transverse plane of the female (panel C) shows the asymmetrical paired mandibles (Md) with the transverse mandibular tendons (TMT), transverse mandibular muscles (TMM1), transverse muscles of mandibles (TMM2), and the posterior rotator muscles of mandibles (PRM). Inset of panel C displays several hemocytes (H) outlined by dotted circles. The transverse plane of male (panel F) displays the paired copulatory hooks (CH) on the first thoracic limbs (T1) and the thickening of the carapace (arrows) at the ventral opening. This also shows the abundance of fat cells (FC) which are quite different from those in the female. Panel F', slightly above that of panel F, shows the pigmented ocellus (O) is connected to the cerebral ganglion (CG). A1M, antennule muscle; A2M, antennal muscle; Ae, aethetascs; An, anus; Ce, hepatic cecum; Cp, carapace; DLM, dorsal longitudinal muscle; ES, end sac of the maxillary gland; FG, food groove; Ht, heart; LGC, labral gland cell; NC, nerve chord; PA, postabdomen; PCAM, posterior carapace adductor muscle; PM, peritrophic membrane; Ra, ramus of swimming antenna; Tu, tubule of the maxillary gland; VLM, ventral longitudinal muscle.

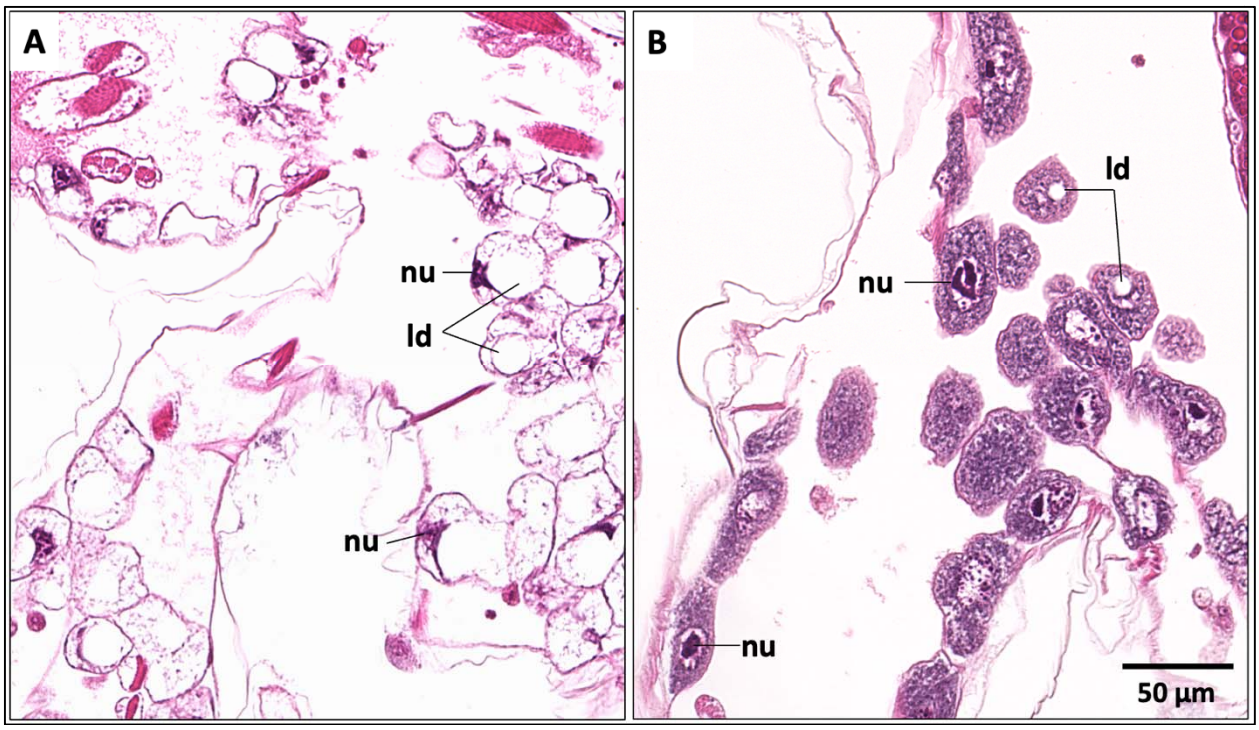

Figure 4. Comparison of male and female fat cells. (A) Fat cells in males consist of larger lipid droplets (ld), reduced and less granular cytoplasm with smaller nucleoli (nu) situated at the cell periphery. **(B)** Fat cells in females have more granular cytoplasm with smaller lipid droplets (ld) and bigger nucleoli (nu) often appeared subdivided and situated in the cell centers.

Circulatory system. *Daphnia* have an open circulatory system and a myogenic heart (63,64). As *Daphnia* are semi-transparent, the beating heart can be easily observed. Hemolymph (blood-like fluid) containing hemocytes (Figure 3C inset) (45,59) is pumped through the body cavity. In line with literature records, we observe that the *Daphnia* heart has a pair of ostia situated in the immediate anterior of the brood chamber, between the midgut and the dorsal surface (Figure 3B, 6C, 6F). Synthesis of hemoglobin happens in fat cells and epipodite cells (on thoracic limbs)(53).

Digestive system. *Daphnia* are filter feeders. Food particles are filtered through filter plates (FP3 and FP4) consisting of setae on thoracic limbs 3 and 4, passed through maxillules and mandibles into the esophagus, which is the first part of the digestive system (Figure 3A and B). The digestive system also consists of paired hepatic ceca, midgut, and hindgut (Figures 6A-C, 6E-F) that are lined with epithelial cells and microvilli, with the columnar epithelial cells in the midgut, and the cuboidal cells in hepatic ceca and hindgut (61,65). The labrum houses labral glands that have been suggested to be involved in food ingestion and endocrine function (69,70) (Figure 3B-D).

306

307 *Excretory system.* The maxillary gland, also known as the shell gland, is the organ of excretion,
308 housed between the inner and outer walls of the carapace (62). It consists of an end sac, a series
309 of tubules, and an opening that is situated within the anterior part of the brood chamber (Figure
310 3A, C, D and F).

311

312 *Locomotive and osmoregulation system.* The second pair of antennae, usually referred to as
313 swimming antennae, is the primary organ of locomotion (43). Each swimming antenna has a
314 protopodite, two rami bearing setae (44) (Figure 3C, D, and F), and is supported by antennal
315 muscles. *Daphnia* have five thoracic limbs (47) (Figure 3B, D, and E). Movements of thoracic
316 limbs produce a constant current that brings food particles into the digestive tract (43,46) and
317 facilitates osmotic regulation, which occurs in the epipodite on each thoracic limb (56). First
318 thoracic limbs in male are different from the female *Daphnia*, with only the male having the
319 chitinized copulatory hooks (Figure 3F) and longer setae (Figure 3E).

320

321 *Muscular system.* The muscular system is very prominent and occupies a significant portion of
322 the body (43,48). The largest muscles are ventral and dorsal longitudinal muscles that extend
323 along the gut, three paired antennal muscles, transverse mandibular muscles, transverse muscles
324 of mandibles, posterior rotator of the mandibles, carapace adductor muscles, followed by groups
325 of muscles that allow the motion of thoracic limbs and postabdomen (Figure 3). Other small
326 muscles include those around the compound eye, labrum, and esophagus (50). All muscles are
327 striated and surrounded by sarcoplasm, which contains many nuclei and is mostly vacuolated.
328 Sarcoplasm is particularly abundant and more vacuolated in the antennal muscles. Male
329 antennules also carry muscles (Figure 3D) that are absent in the females.

330

331 *Nervous, sensory, and vision systems. Daphnia* have a pigmented compound eye consisting of 22
332 ommatidia (Figure 3B) and a light-sensing, pigmented nauplius eye or ocellus with four lens-like
333 bodies (Figure 3F') (66). Each ommatidium contains eight retinular cells sending a parallel
334 bundle of axons, collectively as the optic nerve into the optic lobe, which is then connected to the
335 cerebral ganglia (Figure 3B). The cerebral ganglia are connected to two chains of nerve cords
336 that run along the thorax, underneath the gut, and reach other anatomical structures (57,58)

(Figure 3A, E, and F). Both sexes have a pair of antennules bearing a group of 9 olfactory setae or aesthetascs (71,72) but the male antennules are more prominent and elongated, uniquely fitted with flagella at their tips (Figure 3D').

Reproductive system. The ovaries in females are paired tubular structures ended with oviducts (Figure 3A). *Daphnia* are cyclical parthenogens, which means that sexual (meiotic) and clonal (ameiotic) reproduction alternate (73). Under favorable environmental conditions, females produce parthenogenetic eggs that are genetically identical to themselves. During clonal reproduction, happens in clusters where each cluster of four oocytes are formed. Only one definitive oocyte will accumulate yolk granules and lipid droplets during maturation and the others will transform into nurse cells (60) (Figure 5A). After maturation, parthenogenetic eggs (Figure 5A) are released into the brood chamber through oviducts and fully developed, free-swimming juveniles are extruded after 3 to 4 days. Sexual reproduction is cued by environmental change, such as photoperiod, temperature, and over-crowding, which triggers the parthenogenetic production of genetically identical males for mating with receptive females for sexual recombination; the end point are two embryos that ultimately enter a state of diapause. Unlike parthenogenetic embryos, the development of these resting embryos is arrested at the 3000-cell count and enters dormancy (74). The resting embryos are encased in a chitin shell called an ephippium that protects them from harsh environmental conditions (Figure 5C) including freezing and desiccation. Dormancy in *Daphnia* can be exceptionally long, lasting decades and even centuries (75,76). The resting embryos hatch when cued by favorable environmental conditions. A proportion of these resting embryos is not exposed to environmental cues and remains buried in lake sediment, from where it can be isolated, revived and maintained in the laboratory through parthenogenetic reproduction (77,78).

Testes of male *Daphnia* consist of two long tubular structures connected to gonopores or ejaculatory openings by sperm ducts (Figure 3D and E). Spermatogenesis begins at the testes' walls, and mature spermatozoa are displaced inward toward the central region of the testes (67).

Fat cells, which are polyploid (79) and consist of a massive portion of lipid and glycogen (68), are typically found along the trunk, around ovaries or testes, and on the epipodites of the thoracic

limbs (Figure 3). They are most likely sites of vitellogenin synthesis (68). In the females, these cells contain one or several lipid droplets of various size and one large nucleolus of irregular shape, which often appears sub divided into two or more pieces. Compared to the female fat cells, male fat cells contain much larger lipid droplet, reduced and less granular cytoplasm, and a smaller nucleolus that usually is situated at the cell periphery (Figure 4).

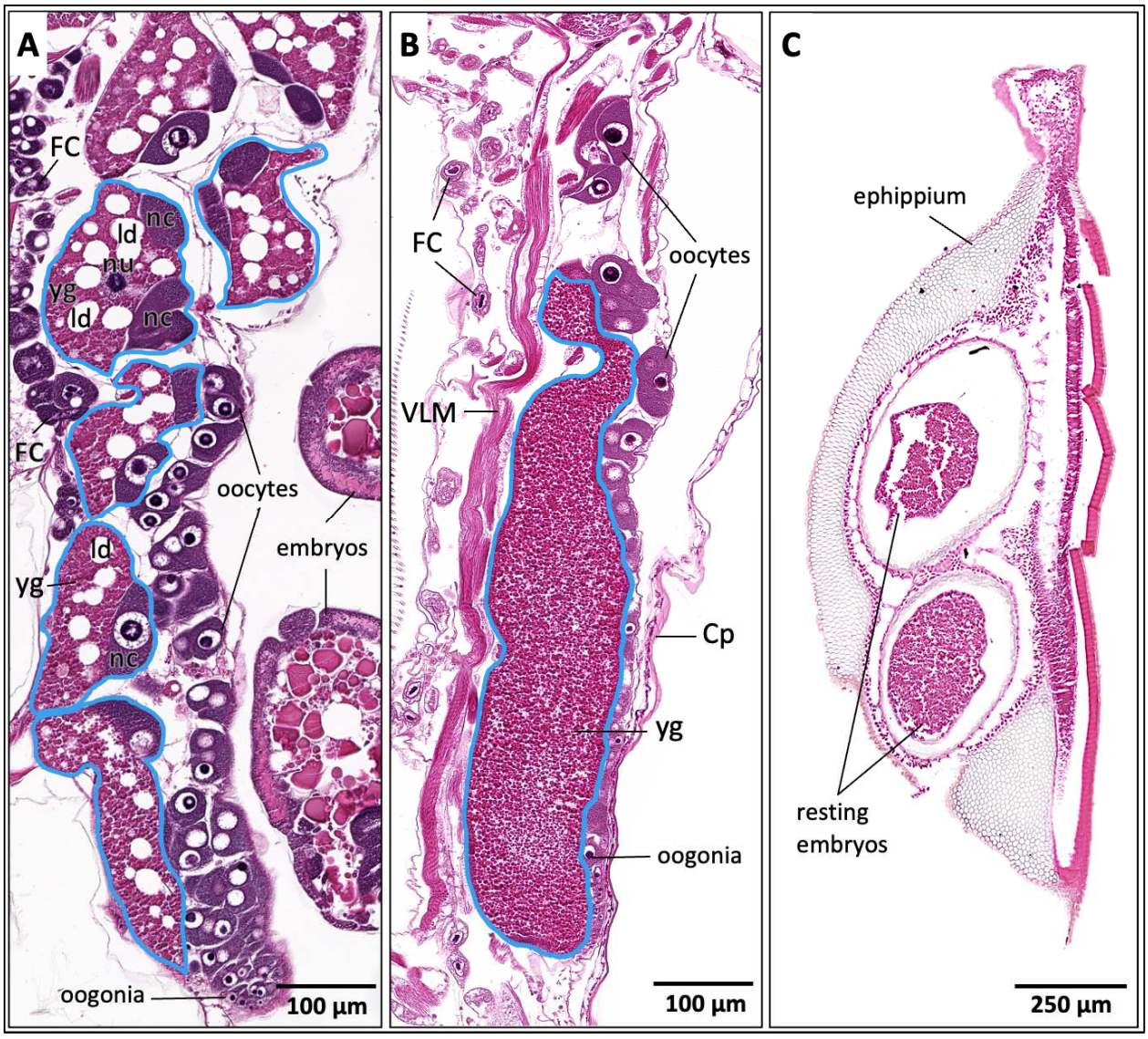

Figure 5. Comparison of parthenogenetic and sexual eggs. (A) The parthenogenetic eggs contain a large amount of lipid droplets (ld) and yolk granules (yg). **(B)** The sexual eggs contain a large proportion of fine yolk granules without lipid droplets. **(C)** Resting embryos encased in the ephippium. Top embryo shows artifact. Cp, carapace; FC, fat cells; nc, nurse cell; nu, the nucleus of oocyte; VLM, ventral longitudinal muscle. A solid blue circle indicates an individual egg.

3.1.3 Documenting histopathological change using DaHRA

To illustrate a key application of the DaHRA, we included a female *D. magna* exposed to acetaminophen to demonstrate toxicity effects across multiple organs and tissue types. We compared tissue architecture in clonal replicates of an exposed and non-exposed *D. magna* to identify pathological tissue phenotypes linked to chemical exposure.

Adult gravid *D. magna* exposed to 25 mg/L of acetaminophen for 72 h produced dead or abnormal embryos. Specifically, the abnormal embryos remained in the chorion, showed development of the compound eye and the gut precursor, but no visible elongation of body length, or development of the swimming antennae and thoracic limbs (Figure 6E) after 72h in the brood chamber.

Histology of the exposed *Daphnia* also revealed changes in various organs and cell types. Vacuoles were observed in most fat cells (Figure 6H) and across the digestive system, including the labral glands (Figure 6F), midgut (Figure 6G) and hindgut (Figure 6H). The midgut and hindgut of the exposed *D. magna* also showed excessive protruding and sloughing of degenerated epithelial cells (Figure 6G and H).

Typically, toxicological effects are quantified through apical endpoints (e.g. immobilization) in acute exposures (80,81) and fitness-linked life history traits in chronic exposures (82,83). Few studies employ ultrastructural analysis of a target organ, usually the midgut, for the histopathological assessment of chemical toxicity (85–88). Sublethal concentration of non-steroidal drugs have previously been shown to reduce reproduction, growth and to induce neurotoxicity in *Daphnia* (89–91). Furthermore, acetaminophen has been shown to induce age-dependent alterations of gene expression and dysregulation of metabolic pathways (92,93). The tissue toxicity we observe in the adult *D. magna* and its embryos confirms these published results, highlighting impact on multiple tissues, as well as embryonic failure.

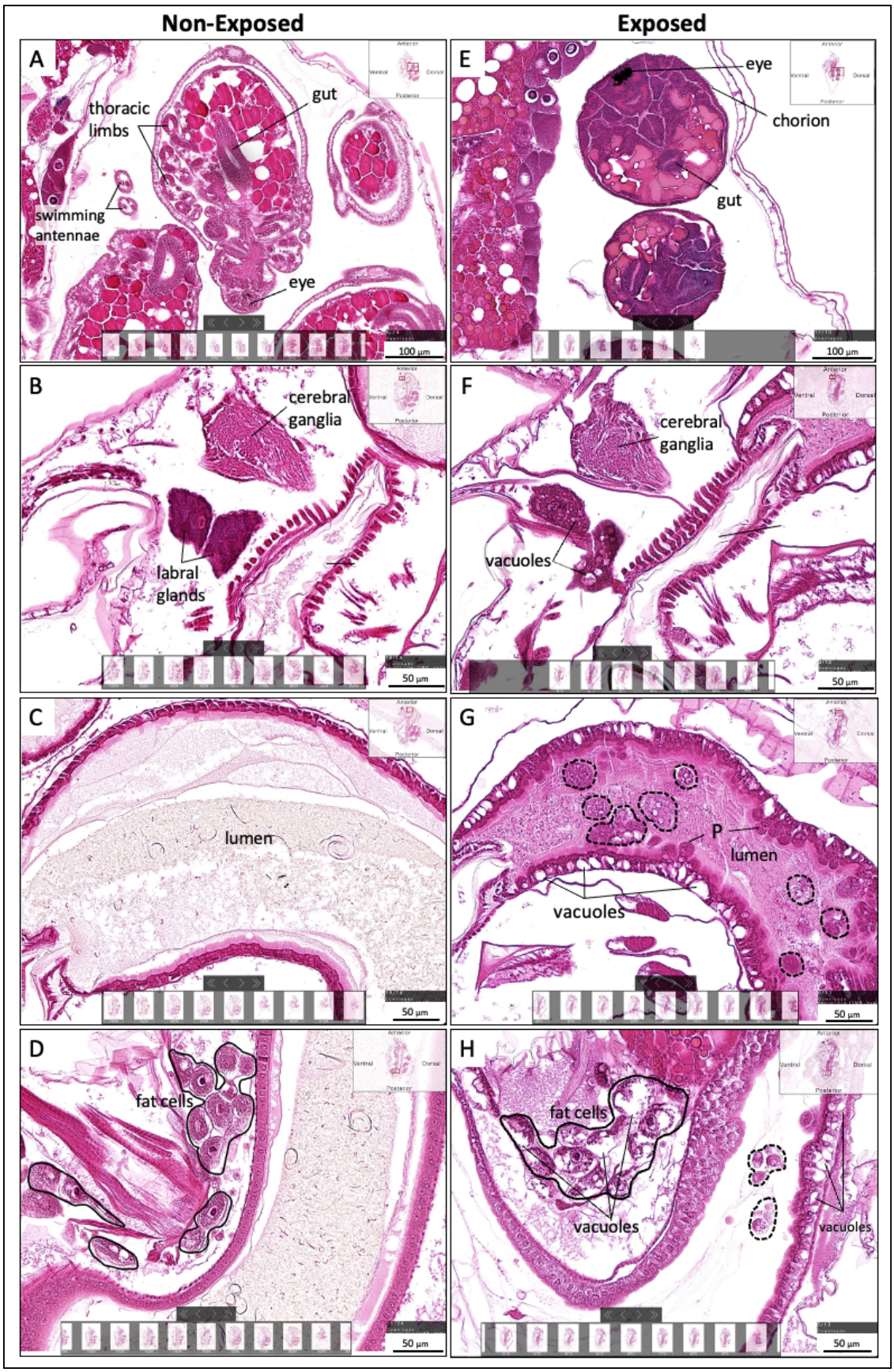

409

Figure 6. Organ and tissue changes in *D. magna* exposed to acetaminophen (E-H) as compared to a clonal replicate of the same non-exposed strain (A-D). (E) Malformed embryos with some development of the compound eye and gut precursors but no visible development of the swimming antennae and thoracic limbs. **(F)** Vacuoles in the labral glands. **(G)** Vacuoles, excessive amount of protruding (P) and sloughing of degenerated epithelial cells (dotted circles) in the midgut of exposed *D. magna*. **(H)** Alteration observed in the fat cells at the postabdomen region; vacuoles, excessive protruding and sloughing of degenerated epithelial cells (dotted circles) in the hindgut.

3.2 Method development for *Daphnia* histology

Invertebrates, especially chitinous aquatic invertebrates are challenging to handle for histology, because of their high tissue water content and the exoskeleton, which has a different texture and composition than soft tissue. We present here key adaptations of histology methods to *D. magna*, paving the way to application in other chitinous invertebrates.

Sample fixation. The accurate representation of microanatomy depends upon the preservation of tissue structure with minimal distortion and optimal staining allowing a clear distinction between cell types and subcellular structures. To determine how to generate sections with minimal distortions for the atlas, we tested three commonly used fixatives: Bouin's solution, 4% Paraformaldehyde in 0.1M phosphate buffer (PFA), and 10% Neutral Buffered Formalin (NBF). Bouin's and PFA are commonly used to fix *D. magna*. NBF was also tested because it is the most used fixative for routine histology of mammalian tissues. The observation of tissue obtained from these three fixatives showed the clearest results with minimal distortion when samples were fixed with Bouin's solution at room temperature for 48 hours. This fixative preserved soft tissues, such as the gut, which are more challenging to maintain intact and allowed us to visualize microvilli and epithelial cell nuclei distinctively (Figure 7A). Nurse cells (nc), oocytes (oo) and yolk granules (yg) were observed intact in the ovaries (Figure 7B) and cellular features across the developing embryos (Figure 7C) were also more clearly visible in samples fixed with Bouin's as compared to PFA and NBF.

The *D. magna* samples (N=23) fixed using PFA and NBF showed "ballooning", a severe fixation artifact causing the carapace to 'puff-up' (Supplementary Figure 2). Inconsistent tissue preservation and distortion in some microanatomical structures were also observed when using

443 these fixatives Particularly, the epithelial cells were not as distinct as when using the Bouin's
444 fixative, and the microvilli were generally not visible in the gut (Figure 7D and 7G). In the
445 ovaries, oocytes and nurse cells were compromised and challenging to be identified due to the
446 tissue damage (Figure 7E and 7H). The developing embryos also showed less cell clarity (Figure
447 7H and 7I). In sum, Bouin's solution was observed to be the best fixative for *D. magna* whole-
448 organism histology and was used to fix all samples used in this atlas.

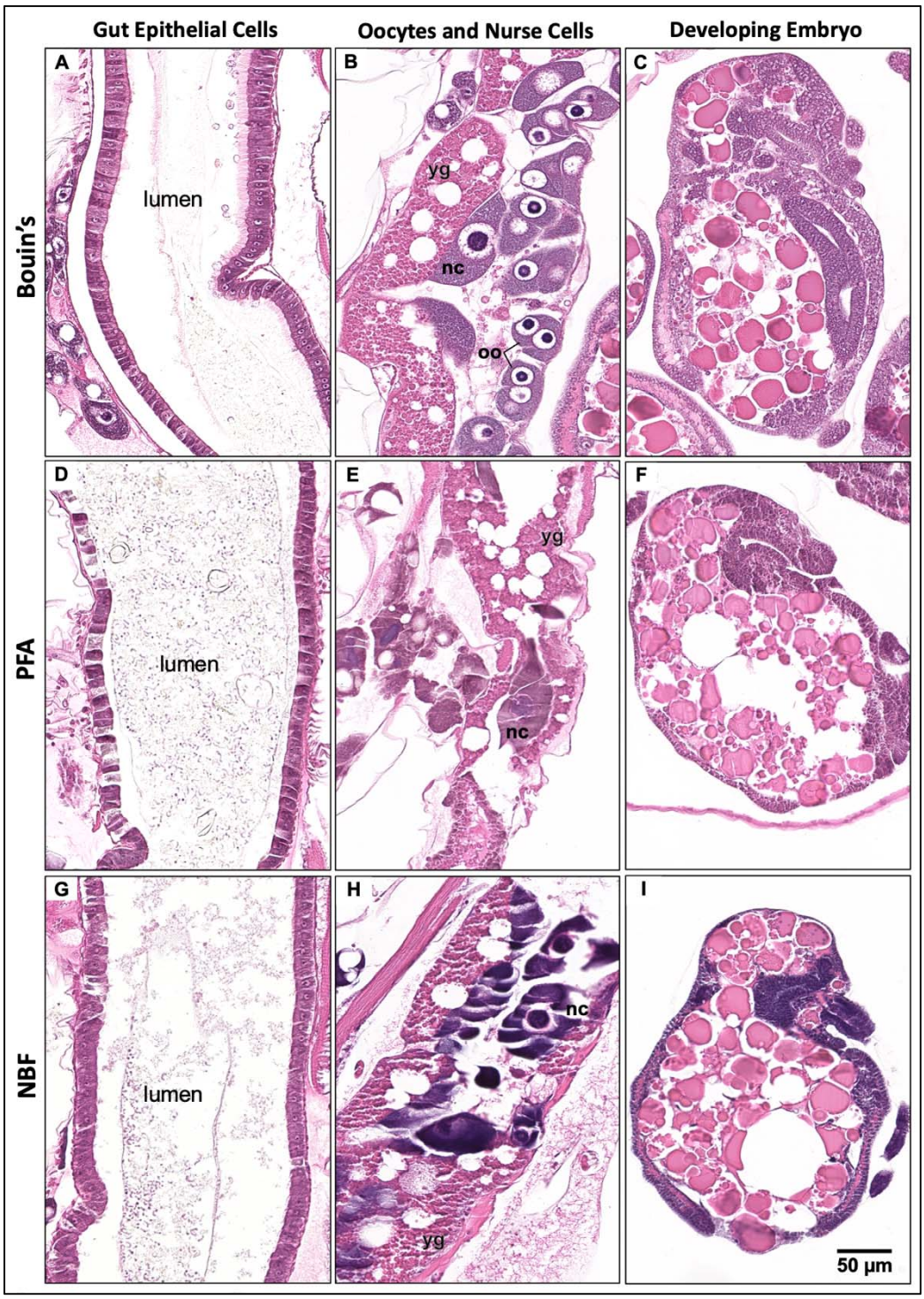

Figure 7. Comparison of histological sections generated with different fixatives: Bouin's, PFA and NBF. Bouin's fixed samples showing intact gut sections, with microvilli and epithelial cell nuclei **(A)**, as well as nurse cells (nc), oocytes (oo) and yolk granules (yg) clearly visible in the ovary **(B)**. In comparison, PFA or NBF fixed samples show less cellular clarity due to the low preservation of histological sections. Cellular details across the developing embryos are clearly visible in samples fixed with Bouin's **(C)** as compared to other two fixatives **(F and I)**.

Sample embedding. Visualization of anatomical sections in each of the three standard anatomical planes (coronal, sagittal, and transverse) is critical for understanding organismal anatomy. Therefore, the ability to generate consistent sections in each of these planes is essential. Agarose pre-embedding using mold or array facilitates consistent positioning and orientation of millimeter-size samples for sectioning (37,38). We have applied this criterion to *D. magna* sections, using custom-designed plastic mold to create agarose blocks with wells that hold individual fixed *D. magna* samples prior to tissue processing and paraffin embedding. We tested several designs of casting molds (Supplementary Figure 3) and found that agarose blocks cast using triangular mold (Figure 8, STL file in Supplementary File 2) allowed consistent and precise positioning of adult *D. magna* samples (see Materials and Methods for details). Using the mold for agarose pre-embedding, we were able to embed up to 18 samples per paraffin block for sectioning.

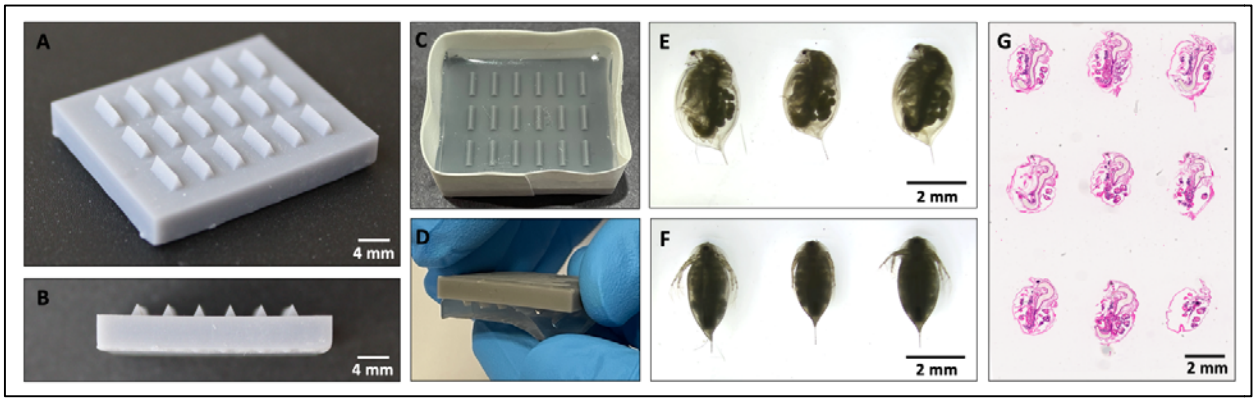

Figure 8. Agarose embedding using casting mold. **(A)** Top view and **(B)** side view of triangular mold printed by stereo-lithography (3D-SLA) at 25 µm resolution for a smooth surface allowing easy removal of agarose blocks. **(C)** Casting 1% agarose block in the taped mold. **(D)** Agarose block is removed from the mold after solidification by peeling the gel downwards. *D. magna* samples laid on their sides with a swimming antenna in the wells **(E)**, the rostra facing the same direction for sagittal plane sectioning and positioned in the wells on their back **(F)** for coronal and transverse plane sectioning. **(G)** Histological section showing the position of samples at sagittal plane.

In summary, to date, *D. magna* lacked comprehensive and annotated histology resources, despite its regulatory importance as a sentinel of environmental hazards and as a model in ecology, and evolution. Our open-source visualization platform for *D. magna* histology with its user-friendly interface that will help the utilization of this tool by non-specialists and students, contributing to

the growing resources for ecotoxicogenomics, biology and comparative medicine. Our atlas provides detailed high-resolution information on tissue-specific phenotypes thereby offering unprecedented opportunities to identify tissue-specific toxicity and genotype-phenotype associations. The coupling of histopathological data with tissue-specific biomarkers (e.g., single cell and spatial transcriptomics) has the potential to revolutionize the assessment of hazardous substances in non-targeted species based on knowledge of the chemical modes of action. Using functional conservation of gene and metabolite network across species, the atlas can assist in revealing tissues target of chemical toxicity across species, including humans (94,95). The pipeline of our atlas was designed with the capability to expand the ontology as more cell or tissue being identified and labeled, and with the intent to extend its features to the other model species. Our ambition is to contribute to the call for cross-species atlas which will be a key resource for the assessment of phenotypes and diseases (96).

Supporting Information

Supplementary Table 1. Fixatives and fixation parameters tested for best preservation of whole *D. magna* samples

Supplementary Table 2. Tissue processing steps for serial dehydration and infiltration of *D. magna* samples with Formula R paraffin in tissue processor

Supplementary Table 3. Automated steps for staining *D. magna* 5-µm sections with Harris' hematoxylin and eosin in an auto-stainer

Supplementary Figure 1. Anatomy of adult male and female *D. magna*

Supplementary Figure 2. "Ballooning" artifact observed in *D. magna* sample fixed with 4% PFA and 10% NBF

Supplementary Figure 3. 3D-SLA printed casting molds of different teeth designs that were tested for orientation and positioning of *Daphnia* samples

Supplementary Text 1. Daphnia anatomy glossary

Supplementary File 1. Anatomical ontology for DaHRA

Supplementary File 2. STL file of casting mold with triangular teeth

Acknowledgments

The authors thank Debra Shearer and Chadwick Harris for sectioning the paraffin blocks and staining the slides. The authors also thank Patrick Leibich and the Department of Surgery, Penn State College of Medicine for 3D-SLA printing the casting molds. This work was supported by the Penn State Human Health and Environment Seed Grant funded by Pennsylvania Department of Health Commonwealth Universal Research Enhancement Program Grant (to KCA) and the National Institutes of Health (1R24OD18559 to KCC), the Jake Gittlen Laboratories for Cancer Research. The Department of Health specifically disclaims responsibility for any analyses, interpretations, or conclusions. This work contributes to the PrecisionTox project (https://precisiontox.org/) that received funding from the European Union's Horizon 2020 research and innovation program under grant agreement No 965406. This output reflects only the author's view, and the European Union cannot be held responsible for any use that may be made of the information contained therein.

Competing Interests

The authors declare no competing interest.

References

1. Fuller R, Landrigan PJ, Balakrishnan K, Bathan G, Bose-O'Reilly S, Brauer M, et al. Pollution and health: a progress update. Lancet Planet Health. 2022 Jun 1;6(6):e535–47.

2. Landrigan PJ, Fuller R, Acosta NJR, Adeyi O, Arnold R, Basu N (Nil), et al. The Lancet Commission on pollution and health. The Lancet. 2018 Feb 3;391(10119):462–512.

3. Naidu R, Biswas B, Willett IR, Cribb J, Kumar Singh B, Paul Nathanail C, et al. Chemical pollution: A growing peril and potential catastrophic risk to humanity. Environ Int. 2021 Nov 1;156:106616.

4. Cardinale BJ, Duffy JE, Gonzalez A, Hooper DU, Perrings C, Venail P, et al. Biodiversity loss and its impact on humanity. Nature. 2012 Jun;486(7401):59–67.

5. Stucki AO, Barton-Maclaren TS, Bhuller Y, Henriquez JE, Henry TR, Hirn C, et al. Use of new approach methodologies (NAMs) to meet regulatory requirements for the assessment of industrial chemicals and pesticides for effects on human health. Front Toxicol [Internet].

2022 [cited 2024 Feb 21];4. Available from: https://www.frontiersin.org/articles/10.3389/ftox.2022.964553

6. Harrill JA, Viant MR, Yauk CL, Sachana M, Gant TW, Auerbach SS, et al. Progress towards an OECD reporting framework for transcriptomics and metabolomics in regulatory toxicology. Regul Toxicol Pharmacol RTP. 2021 Oct;125:105020.

7. Hines A, Staff FJ, Widdows J, Compton RM, Falciani F, Viant MR. Discovery of metabolic signatures for predicting whole organism toxicology. Toxicol Sci Off J Soc Toxicol. 2010 Jun;115(2):369–78.

8. Palmer JA, Smith AM, Gryshkova V, Donley ELR, Valentin JP, Burrier RE. A Targeted Metabolomics-Based Assay Using Human Induced Pluripotent Stem Cell-Derived Cardiomyocytes Identifies Structural and Functional Cardiotoxicity Potential. Toxicol Sci. 2020 Apr;174(2):218–40.

9. European Chemicals Agency. The use of alternatives to testing on animals for the REACH Regulation [Internet]. European Chemicals Agency; 2020. Available from: https://data.europa.eu/doi/10.2823/092305

10. HOME - PrecisionTox [Internet]. [cited 2024 Feb 21]. Available from: https://precisiontox.org/

11. Ebert D. Daphnia as a versatile model system in ecology and evolution. EvoDevo. 2022 Aug 8;13(1):16.

12. Miner BE, De Meester L, Pfrender ME, Lampert W, Hairston NG. Linking genes to communities and ecosystems: Daphnia as an ecogenomic model. Proc R Soc B Biol Sci. 2012 May 22;279(1735):1873–82.

13. Stollewerk A. The water flea Daphnia - a “new” model system for ecology and evolution? J Biol. 2010 Jan 13;9(2):21.

14. Cuenca-Cambronero M, Pantel JH, Marshall H, Nguyen TTT, Tomero-Sanz H, Orsini L. Evolutionary mechanisms underpinning fitness response to multiple stressors in Daphnia. Evol Appl. 2021;14(10):2457–69.

15. Stoks R, Govaert L, Pauwels K, Jansen B, De Meester L. Resurrecting complexity: the interplay of plasticity and rapid evolution in the multiple trait response to strong changes in predation pressure in the water flea Daphnia magna. Ecol Lett. 2016;19(2):180–90.

16. Walsh MR, Packer M, Beston S, Funkhouser C, Gillis M, Holmes J, et al. Daphnia as a Model for Eco-evolutionary Dynamics. In: Thiel M, Wellborn GA, editors. Life Histories: Volume 5 [Internet]. Oxford University Press; 2018 [cited 2024 Jan 3]. p. 0. Available from: https://doi.org/10.1093/oso/9780190620271.003.0016

17. Hebert PDN, Ward RD. Inheritance during parthenogenesis in Daphnia magna. Genetics. 1972 Aug;71(4):639–42.

18. Kim HJ, Koedrith P, Seo YR. Ecotoxicogenomic approaches for understanding molecular mechanisms of environmental chemical toxicity using aquatic invertebrate, Daphnia model organism. Int J Mol Sci. 2015 May 29;16(6):12261–87.

19. Shaw JR, Pfrender ME, Eads BD, Klaper R, Callaghan A, Sibly RM, et al. Daphnia as an emerging model for toxicological genomics. In: Hogstrand C, Kille P, editors. Advances in Experimental Biology [Internet]. Elsevier; 2008 [cited 2021 Oct 8]. p. 165–328. (Comparative Toxicogenomics; vol. 2). Available from: https://www.sciencedirect.com/science/article/pii/S1872242308000057

20. Chaturvedi A, Li X, Dhandapani V, Marshall H, Kissane S, Cuenca-Cambronero M, et al. The hologenome of Daphnia magna reveals possible DNA methylation and microbiome-mediated evolution of the host genome. Nucleic Acids Res. 2023 Aug 28;51(18):9785–803.

21. Byeon E, Kim MS, Kim DH, Lee Y, Jeong H, Lee JS, et al. The freshwater water flea Daphnia magna NIES strain genome as a resource for CRISPR/Cas9 gene targeting: The glutathione S-transferase omega 2 gene. Aquat Toxicol. 2022 Jan 1;242:106021.

22. Lee BY, Choi BS, Kim MS, Park JC, Jeong CB, Han J, et al. The genome of the freshwater water flea Daphnia magna: A potential use for freshwater molecular ecotoxicology. Aquat Toxicol. 2019 May 1;210:69–84.

23. Campos B, Fletcher D, Piña B, Tauler R, Barata C. Differential gene transcription across the life cycle in Daphnia magna using a new all genome custom-made microarray. BMC Genomics. 2018 May 18;19:370.

24. Jankowski MD, Fairbairn DJ, Baller JA, Westerhoff BM, Schoenfuss HL. Using the Daphnia magna Transcriptome to Distinguish Water Source: Wetland and Stormwater Case Studies. Environ Toxicol Chem. 2022 Sep;41(9):2107–23.

25. Orsini L, Gilbert D, Podicheti R, Jansen M, Brown JB, Solari OS, et al. Daphnia magna transcriptome by RNA-Seq across 12 environmental stressors. Sci Data. 2016 May 1;3:160030.

26. Majno G, Joris I. Cells, tissues, and disease□: principles of general pathology. 2nd ed. New York□: Oxford University Press; 2004. 1005 p.

27. Wester PW, Canton JH. The usefulness of histopathology in aquatic toxicity studies. Comp Biochem Physiol Part C Comp Pharmacol. 1991 Jan 1;100(1):115–7.

28. Huang J, Wang Q, Liu S, Zhang M, Liu Y, Sun L, et al. Crosstalk between histological alterations, oxidative stress and immune aberrations of the emerging PFOS alternative OBS in developing zebrafish. Sci Total Environ. 2021 Jun 20;774:145443.

29. Manjunatha B, Seo E, Bangyappagari D, Lee SJ. Histopathological and ultrastructural alterations reveal the toxicity of particulate matter (PM2.5) in adult zebrafish. J Hazard Mater Adv. 2022 Aug 1;7:100135.

30. Ramírez-Duarte W, Rondon Barragan I, Eslava-Mocha P. Acute toxicity and histopathological alterations of Roundup® herbicide on “cachama blanca” (Piaractus brachypomus). Pesqui Veterinária Bras. 2008 Nov 1;28:547.

31. Fraga N, Benito D, Briaudeau T, Izagirre U, Ruiz P. Toxicopathic effects of lithium in mussels. Chemosphere. 2022 Nov 1;307:136022.

32. Joshy A, Sharma SRK, Mini KG, Gangadharan S, Pranav P. Histopathological evaluation of bivalves from the southwest coast of India as an indicator of environmental quality. Aquat Toxicol. 2022 Feb 1;243:106076.

33. Phong Vo HN, Le GK, Hong Nguyen TM, Bui XT, Nguyen KH, Rene ER, et al. Acetaminophen micropollutant: Historical and current occurrences, toxicity, removal strategies and transformation pathways in different environments. Chemosphere. 2019 Dec;236:124391.

34. Perananthan V, Shihana F, Chiew AL, George J, Dawson A, Buckley NA. Intestinal injury in paracetamol overdose (ATOM-8). J Gastroenterol Hepatol. 2023 Dec 27;

35. Yoon E, Babar A, Choudhary M, Kutner M, Pyrsopoulos N. Acetaminophen-Induced Hepatotoxicity: a Comprehensive Update. J Clin Transl Hepatol. 2016 Jun 28;4(2):131–42.

36. Zhang L, Baer KN. The influence of feeding, photoperiod and selected solvents on the reproductive strategies of the water flea, Daphnia magna. Environ Pollut. 2000 Dec 1;110(3):425–30.

37. Copper JE, Budgeon LR, Foutz CA, van Rossum DB, Vanselow DJ, Hubley MJ, et al. Comparative analysis of fixation and embedding techniques for optimized histological preparation of zebrafish. Comp Biochem Physiol Toxicol Pharmacol CBP. 2018 Jun;208:38–46.

38. Santana LMBM, Damasceno ÉP, Loureiro S, Soares AMVM, Pousão-Ferreira P, Abessa DMS, et al. An Easy-to-Use Histological Technique for Small Biological Samples of Senegalese Sole Larvae. Appl Sci. 2023 Jan;13(4):2346.

39. Sabaliauskas NA, Foutz CA, Mest JR, Budgeon LR, Sidor AT, Gershenson JA, et al. High-throughput zebrafish histology. Methods. 2006 Jul 1;39(3):246–54.

40. Copper JE, Budgeon LR, Foutz CA, van Rossum DB, Vanselow DJ, Hubley MJ, et al. Comparative analysis of fixation and embedding techniques for optimized histological preparation of zebrafish. Comp Biochem Physiol Part C Toxicol Pharmacol. 2018 Jun 1;208:38–46.

41. Schindelin J, Arganda-Carreras I, Frise E, Kaynig V, Longair M, Pietzsch T, et al. Fiji: an open-source platform for biological-image analysis. Nat Methods. 2012 Jul;9(7):676–82.

42. Schneider CA, Rasband WS, Eliceiri KW. NIH Image to ImageJ: 25 years of image analysis. Nat Methods. 2012 Jul;9(7):671–5.

651 43. Fryer G. Functional morphology and the adaptive radiation of the Daphniidae
652 (Branchiopoda: Anomopoda). Philos Trans R Soc Lond B Biol Sci. 1991 Jan
653 29;331(1259):1–99.

654 44. Agar WE. The swimming setae of Daphnia carinata. J Cell Sci. 1950 Dec 1;s3-91(16):353–
655 68.

656 45. Auld SKJR, Scholefield JA, Little TJ. Genetic variation in the cellular response of Daphnia
657 magna (Crustacea: Cladocera) to its bacterial parasite. Proc R Soc B Biol Sci. 2010 Nov
658 7;277(1698):3291–7.

659 46. Bednarska A. Adaptive changes in morphology of Daphnia filter appendages in response to
660 food stress. Polish Journal of Ecology. 2006;54:663–8.

661 47. Benzie JAH. The Genus Daphnia (including Daphniopsis) (Anomopoda:Daphniidae).
662 Kenobi Productions; 2005. 388 p.

663 48. Binder G. Das Muskelsystem von Daphnia. Int Rev Gesamten Hydrobiol Hydrogr.
664 1931;26(1–2):54–98.

665 49. Christensen AK, Owusu NG, Jean-Louis D. Carapace epithelia are rich in large filamentous
666 actin bundles in Daphnia magna, Daphnia pulex, and Sida crystallina (Crustacea:
667 Cladocera). Invertebr Biol. 2018;137(1):49–59.

668 50. Consi TR, Macagno ER, Necles N. The oculomotor system of Daphnia magna. The eye
669 muscles and their motor neurons. Cell Tissue Res. 1987 Mar;247(3):515–23.

670 51. Ebert D. Introduction to Daphnia Biology [Internet]. Ecology, Epidemiology, and Evolution
671 of Parasitism in Daphnia [Internet]. National Center for Biotechnology Information (US);
672 2005 [cited 2021 Mar 14]. Available from: https://www.ncbi.nlm.nih.gov/books/NBK2042/

673 52. Edwards C. The anatomy of Daphnia mandibles. Trans Am Microsc Soc. 1980;99(1):2–24.

674 53. Goldmann T, Becher B, Wiedorn KH, Pirow R, Deutschbein ME, Vollmer E, et al. Epipodite
675 and fat cells as sites of hemoglobin synthesis in the branchiopod crustacean Daphnia
676 magna. Histochem Cell Biol. 1999 Nov;112(5):335–9.

677 54. Halcrow K. The fine structure of the carapace integument of Daphnia magna Straus
678 (Crustacea Branchiopoda). Cell Tissue Res. 1976 Jun 14;169(2):267–76.

679 55. Hiruta C, Tochinai S. Formation and structure of the ephippium (resting egg case) in relation
680 to molting and egg laying in the water flea Daphnia pulex De Geer (Cladocera:
681 Daphniidae). J Morphol. 2014 Jul;275(7):760–7.

682 56. Kikuchi S. The fine structure of the gill epithelium of a fresh-water flea, Daphnia magna
683 (Crustacea: Phyllopoda) and changes associated with acclimation to various salinities. I.
684 Normal fine structure. Cell Tissue Res. 1983;229(2):253–68.

685 57. Kress T, Harzsch S, Dircksen H. Neuroanatomy of the optic ganglia and central brain of the
686 water flea Daphnia magna (Crustacea, Cladocera). Cell Tissue Res. 2016 Mar
687 1;363(3):649–77.

688 58. McCoole MD, Baer KN, Christie AE. Histaminergic signaling in the central nervous system
689 of Daphnia and a role for it in the control of phototactic behavior. J Exp Biol. 2011 May
690 15;214(Pt 10):1773–82.

691 59. Metschnikoff E. A disease of Daphnia caused by a yeast. A contribution to the theory of
692 phagocytes as agents for attack on disease-causing organisms. Archiv Pathol Anat Physiol
693 Klin Med. 1884;96:177–95.

694 60. Rossi F. Comparative observations on the female reproductive system and parthenogenetic
695 oogenesis in Cladocera. Bolletino Zool. 1980 Jan;47(1–2):21–38.

696 61. Schultz TW, Kennedy JR. The fine structure of the digestive system of Daphnia pulex
697 (Crustacea: Cladocera). Tissue Cell. 1976 Jan 1;8(3):479–90.

698 62. Smirnov NN. Physiology of the Cladocera. Physiol Cladocera. 2013 Oct 1;1–336.

699 63. Stein RJ, Richter WR, Zussman RA, Brynjolfsson G. Ultrastructural characterization of
700 Daphnia heart muscle. J Cell Biol. 1966 Apr 1;29(1):168–70.

701 64. Steinsland AJ. Heart ultrastructure in Daphnia pulex De Geer (Crustacea, Branchiopoda,
702 Cladocera). J Crustac Biol. 1982;2(1):54–8.

703 65. Quaglia A, Sabelli B, Villani L. Studies on the intestine of Daphnidae (Crustacea, Cladocera)
704 ultrastructure of the midgut of Daphnia magna and Daphnia obtusa. J Morphol.
705 1976;150(3):711–25.

706 66. Weiss LC, Tollrian R, Herbert Z, Laforsch C. Morphology of the Daphnia nervous system: a
707 comparative study on Daphnia pulex, Daphnia lumholtzi, and Daphnia longicephala. J
708 Morphol. 2012 Dec;273(12):1392–405.

709 67. Wuerz M, Huebner E, Huebner J. The morphology of the male reproductive system,
710 spermatogenesis and the spermatozoon of Daphnia magna (Crustacea: Branchiopoda). J
711 Morphol. 2017 Nov;278(11):1536–50.

712 68. Zaffagnini F, Zeni C. Considerations on some cytological and ultrastructural observations on
713 fat cells of Daphnia (Crustacea, Cladocera). Bollettino di zoologia. 1986;53(1):33–9.

714 69. Zaffagnini F, Zeni C. Ultrastructural investigations on the labral glands of Daphnia obtusa
715 (Crustacea, Cladocera). J Morphol. 1987 Jul;193(1):23–33.

716 70. Zeni C, Franchini A. A preliminary histochemical study on the labral glands of Daphnia
717 obtusa (Crustacea, Cladocera). Acta Histochem. 1990;88:175–81.

718 71. Rieder N. The ultrastructure of the so-called olfactory setae on the antennula of Daphnia
719 magna Straus (Crustacea, Cladocera). In: Forró L, Frey DG, editors. Cladocera. Dordrecht:
720 Springer Netherlands; 1987. p. 175–81. (Developments in Hydrobiology).

721 72. Klann M, Stollewerk A. Evolutionary variation in neural gene expression in the developing
722 sense organs of the crustacean Daphnia magna. Dev Biol. 2017 Apr 1;424(1):50–61.

723 73. Decaestecker E, De Meester L, Mergeay J. Cyclical parthenogenesis in Daphnia: sexual
724 versus asexual reproduction. In: Schön I, Martens K, Dijk P, editors. Lost Sex: The
725 Evolutionary Biology of Parthenogenesis [Internet]. Dordrecht: Springer Netherlands; 2009
726 [cited 2022 Jan 21]. p. 295–316. Available from: https://doi.org/10.1007/978-90-481-2770-
727 2_15

728 74. Chen L, Barnett RE, Horstmann M, Bamberger V, Heberle L, Krebs N, et al. Mitotic activity
729 patterns and cytoskeletal changes throughout the progression of diapause developmental
730 program in Daphnia. BMC Cell Biol. 2018 Dec 29;19:30.

731 75. Cáceres CE. Interspecific variation in the abundance, production, and emergence of Daphnia
732 diapausing eggs. Ecology. 1998;79(5):1699–710.

733 76. Mergeay J, Verschuren D, Kerckhoven LV, Meester LD. Two hundred years of a diverse
734 Daphnia community in Lake Naivasha (Kenya): effects of natural and human-induced
735 environmental changes. Freshw Biol. 2004;49(8):998–1013.

736 77. Arbačiauskas K, Gasiūnaitė ZR. Growth and fecundity of Daphnia after diapause and their
737 impact on the development of a population. Hydrobiologia. 1996 Mar 1;320(1):209–22.

738 78. Cambronero MC, Orsini L. Resurrection of Dormant Daphnia magna: Protocol and
739 Applications. JoVE J Vis Exp. 2018 Jan 19;(131):e56637.

740 79. Beaton MJ, Hebert PDN. Miniature genomes and endopolyploidy in cladoceran crustaceans.
741 Genome. 1989 Dec 1;32(6):1048–53.

742 80. Environmental Protection Agency. Methods for Measuring the Acute Toxicity of Effluents
743 and Receiving Waters to Freshwater and Marine Organisms. 2002.

744 81. OECD. Test No. 202: Daphnia sp. Acute Immobilisation Test [Internet]. Paris: Organisation
745 for Economic Co-operation and Development; 2004 [cited 2021 Nov 4]. Available from:
746 https://www.oecd-ilibrary.org/environment/test-no-202-daphnia-sp-acute-immobilisation-
747 test_9789264069947-en

748 82. Environmental Protection Agency. Ecological Effects Test Guidelines OCSPP850.1300:
749 Daphnid chronic toxicity test. 1996.

750 83. OECD. Daphnia magna Reproduction Test (OECD TG 211) [Internet]. Paris: OECD; 2018
751 Sep [cited 2021 Nov 4] p. 253–63. Available from: https://www.oecd-
752 ilibrary.org/environment/revised-guidance-document-150-on-standardised-test-guidelines-

753 for-evaluating-chemicals-for-endocrine-disruption/daphnia-magna-reproduction-test-oecd-
754 tg-211_9789264304741-12-en

755 84. Tkaczyk A, Bownik A, Dudka J, Kowal K, Ślaska B. Daphnia magna model in the toxicity
756 assessment of pharmaceuticals: A review. Sci Total Environ. 2021 Apr 1;763:143038.

757 85. Bacchetta R, Santo N, Marelli M, Nosengo G, Tremolada P. Chronic toxicity effects of
758 ZnSO4 and ZnO nanoparticles in Daphnia magna. Environ Res. 2017 Jan 1;152:128–40.

759 86. Bodar CWM, van Donselaar EG, Herwig HJ. Cytopathological investigations of digestive
760 tract and storage cells in Daphnia magna exposed to cadmium and tributyltin. Aquat
761 Toxicol. 1990 Oct 1;17(4):325–37.

762 87. Heinlaan M, Kahru A, Kasemets K, Arbeille B, Prensier G, Dubourguier HC. Changes in the
763 Daphnia magna midgut upon ingestion of copper oxide nanoparticles: A transmission
764 electron microscopy study. Water Res. 2011 Jan 1;45(1):179–90.

765 88. Yang XY, Edelmann RE, Oris JT. Suspended C60 nanoparticles protect against short-term
766 UV and fluoranthene photo-induced toxicity, but cause long-term cellular damage in
767 Daphnia magna. Aquat Toxicol. 2010 Oct 15;100(2):202–10.

768 89. Daniel D, Dionísio R, de Alkimin GD, Nunes B. Acute and chronic effects of paracetamol
769 exposure on Daphnia magna: how oxidative effects may modulate responses at distinct
770 levels of organization in a model species. Environ Sci Pollut Res. 2019 Feb 1;26(4):3320–9.

771 90. Du J, Mei CF, Ying GG, Xu MY. Toxicity Thresholds for Diclofenac, Acetaminophen and
772 Ibuprofen in the Water Flea Daphnia magna. Bull Environ Contam Toxicol. 2016
773 Jul;97(1):84–90.

774 91. de Oliveira LLD, Antunes SC, Gonçalves F, Rocha O, Nunes B. Acute and chronic
775 ecotoxicological effects of four pharmaceuticals drugs on cladoceran Daphnia magna. Drug
776 Chem Toxicol. 2016;39(1):13–21.

777 92. Heckmann LH, Connon R, Hutchinson TH, Maund SJ, Sibly RM, Callaghan A. Expression
778 of target and reference genes in Daphnia magna exposed to ibuprofen. BMC Genomics.
779 2006 Dec;7(1):175.

780 93. Lari E, Jeong TY, Labine LM, Simpson MJ. Metabolomic analysis predicted changes in
781 growth rate in Daphnia magna exposed to acetaminophen. Aquat Toxicol Amst Neth. 2022
782 Aug;249:106233.

783 94. Abdullahi M, Li X, Abdallah MAE, Stubbings W, Yan N, Barnard M, et al. Daphnia as a
784 Sentinel Species for Environmental Health Protection: A Perspective on Biomonitoring and
785 Bioremediation of Chemical Pollution. Environ Sci Technol. 2022 Oct 18;56(20):14237–
786 48.

787 95. Colbourne JK, Shaw JR, Sostare E, Rivetti C, Derelle R, Barnett R, et al. Toxicity by
788 descent: A comparative approach for chemical hazard assessment. Environ Adv. 2022 Oct
789 1;9:100287.

790 96. Cheng KC, Burdine RD, Dickinson ME, Ekker SC, Lin AY, Lloyd KCK, et al. Promoting
791 validation and cross-phylogenetic integration in model organism research. Dis Model
792 Mech. 2022 Sep 20;15(9):dmm049600.

793 97. Haney JF, Hall DJ. Sugar-coated Daphnia: A preservation technique for Cladocera1. Limnol
794 Oceanogr. 1973;18(2):331–3.

795